Woo-Pyo Hong and Young-Dae Jung*

Multimode Characteristics of Space-Charge Waves in a Plasma Waveguide

DOI 10.1515/zna-2016-0255
Received June 28, 2016; accepted July 26, 2016; previously published online August 25, 2016

Abstract: The multimode characteristics of the space-charge wave are investigated in a cylindrical wave-guide complex plasma. The dispersion relation of the space-charge wave is derived in a waveguide, including two-temperature electrons. The results show that the wave frequencies in a plasma with a high population of high-temperature electrons are always smaller those in a plasma with a low population of high-temperature electrons. It is also found that the population of high-temperature electrons suppresses the group velocity of the space-charge wave. In addition, it is found that the frequency increases with an increase in the radius of the cylindrical wave guide. The variations of the frequency and the group velocity due to the density, temperature, and geometric effects are also discussed.

Keywords: Complex plasma; Multimode propagation; space-charge wave.

1 Introduction

The characteristics of the plasma surface have received considerable attention over the years in various bounded and semibounded plasmas because the surface waves have applications in many areas of modern science and technologies, such as laser physics, materials science, nanotechnology, plasma spectroscopy, and space physics [1, 2]. It is also shown that the propagation of surface plasma waves is important in fusion devices because the surface waves are related to plasma heating and impurity generation [3]. Usually, the Debye-Hückel potential obtained by the linearization of the Poisson equation with the Maxwell-Boltzmann distribution function has been used to express screened interaction potentials in weakly coupled electron-ion plasmas because the average kinetic energy of a plasma particle is greater than the typical magnitude of the interaction energy between plasma particles [4, 5]. Recently, the complex plasmas containing charged aerosol or dust grains are ubiquitous in astrophysical and laboratory dusty plasmas. In addition, the charged dust grains have wide applications in semiconductor devices, quantum dots, and high-tech industries because nano- and microsized dust grains have collective and nonideal effects [6–9]. The propagation of ion-acoustic waves has been investigated in a double-electron-temperature plasma [10]. In addition, the physical properties of ion-acoustic solitary waves were explored in a two-electron-temperature plasma [11]. It has been shown that strong electron-beam-plasma interactions can result in two-electron-temperature distributions because the unstable Langmuir mode due to a nonlinear wave interaction process would be the parametric decay mode into a counterpropagating second Langmuir mode and a forward propagating ion-acoustic wave [10, 12]. It is also shown that there exists an electron-acoustic mode when the plasma electrons have bi-Maxwellian distributions with two different temperatures [13–15]. However, to the best of our knowledge, the physical properties of the space-charge electron-acoustic plasma wave in a cylindrically bounded dusty plasma of two-temperature electrons have not been investigated as yet. Thus, in this paper, we investigate the influence of plasma density and temperature on the space-charge electron-acoustic wave in a cylindrically bounded dusty plasma of two-temperature electrons because the investigation of the plasma wave in the plasma-vacuum interface would provide useful information on the propagation of the electron-acoustic plasma wave and the geometric effect due to the harmonic characteristics of the Bessel functions. It is also expected that the variation of group velocity of space-charge waves due to the change of ratio of the temperature of hot electrons to the temperature of cold electrons provides useful information on the physical characteristics of the space-charge wave in a plasma waveguide, including two-temperature electrons. We obtain the dispersion relation and the group velocity of the space-charge electron-acoustic wave in a

***Corresponding author: Young-Dae Jung,** Department of Electrical and Computer Engineering, MC 0407, University of California, San Diego, 9500 Gilman Drive, La Jolla, California 92093-0407, USA, and Department of Applied Physics and Department of Bionanotechnology, Hanyang University, Ansan, Kyunggi-Do 15588, South Korea, E-mail: ydjung@hanyang.ac.kr; ydjung@gmail.com
Woo-Pyo Hong: Department of Electronics Engineering, Catholic University of Daegu, Hayang 38430, South Korea

cylindrically bounded dusty plasma of two-temperature electrons. The variations of the frequency and the group velocity due to the density, temperature, and geometric effects are also discussed.

In Section 2, we discuss the plasma dielectric function in thermal duty plasmas with two-temperature electrons. We also obtain the dispersion relation for the space-charge electron-acoustic wave for the space-charge electron-acoustic wave in a cylindrically bounded dusty plasma. In Section 3, we obtain the wave frequency and group velocity of the space-charge electron-acoustic wave. Finally, the discussions and conclusion, including the density, temperature, and geometric effects on the frequency and the group velocity of the space-charge electron-acoustic wave in a cylindrically bounded dusty plasma of two-temperature electrons, are given in Section 4.

2 Plasma Dielectric Function and Dispersion Relation

We shall consider a thermal duty plasma encompassing two-temperature electrons, ions, and charged dust grains because it is known that the electron-acoustic mode exists when the plasma electrons have two different temperature distribution functions [15]. In thermal duty plasmas with two-temperature electrons, the longitudinal plasma dielectric function [16] $\varepsilon_l(\omega, k)$ would be obtained by the plasma dielectric susceptibilities $\chi_\alpha(\omega, k)$ for low-temperature electrons ($\alpha=L$), high-temperature electrons ($\alpha=H$), ions ($\alpha=i$), and dust grains ($\alpha=d$):

$$\varepsilon_l(\omega, k)=1+\sum_{\alpha=L,H,i,d}\chi_\alpha(\omega, k)$$
$$=1-\sum_{\alpha=L,H,i,d}\frac{\omega_\alpha^2}{k^2}\int_{-\infty}^{\infty}\mathrm{d}v_z\frac{\partial f_\alpha(v_z)/\partial v_z}{v_z-\omega/k_z}, \quad (1)$$

where ω is the frequency, k is the wave number, $\omega_\alpha[=(4\pi n_\alpha q_\alpha^2/m_\alpha)^{1/2}]$ is the plasma frequency of the species α, n_α is the number density, q_α is the electric charge, m_α is the mass, $f_\alpha(v_z)[=(2\pi v_\alpha^2)^{-1/2}\exp(-v_z^2/2v_\alpha^2)]$ is the distribution function, $v_\alpha[=(k_\mathrm{B}T_\alpha/m_\alpha)^{1/2}]$ is the thermal velocity, k_B is the Boltzmann constant, and T_α is the plasma temperature. In the range of phase velocity ω/k_z, i.e. the electron-acoustic wave domain, $(k_\mathrm{B}T_d/m_d)^{1/2}<(k_\mathrm{B}T_i/m_i)^{1/2}<(k_\mathrm{B}T_\mathrm{L}/m_e)^{1/2}\ll\omega/k_z\ll(k_\mathrm{B}T_\mathrm{H}/m_e)^{1/2}$ with $Z_d\ll m_d/m_i$, where Z_d is the charge number of the dust grain, the plasma dielectric function [13, 15] $\varepsilon_l(\omega, k)$ with two-temperature plasma electrons is given by

$$\varepsilon_l(\omega, k)\cong1+\frac{1}{k^2\lambda_\mathrm{DH}^2}-\frac{\omega_L^2}{\omega^2}\left(1+\frac{3k^2}{\omega^2}\frac{k_\mathrm{B}T_\mathrm{L}}{m_e}\right)-\frac{\omega_i^2}{\omega^2}\left(1+\frac{3k^2}{\omega^2}\frac{k_\mathrm{B}T_i}{m_i}\right)-\frac{\omega_d^2}{\omega^2}, \quad (2)$$

where λ_DH is the Debye length for high-temperature electrons. In unmagnetized dusty plasmas, the continuity and momentum equations for the α species of plasma particle are given by

$$\frac{\partial n_\alpha}{\partial t}+\nabla\cdot(n_\alpha\mathbf{v}_\alpha)=0, \quad (3)$$

$$m_\alpha n_\alpha\left(\frac{\partial\mathbf{v}_\alpha}{\partial t}+\mathbf{v}_\alpha\cdot\nabla\mathbf{v}_\alpha\right)=-\nabla P_\alpha-q_\alpha n_\alpha\nabla\varphi, \quad (4)$$

and Poisson's equation is

$$\nabla^2\varphi=-4\pi\sum_{\alpha=e,i,d}q_\alpha n_\alpha, \quad (5)$$

where $n_\alpha=n_{\alpha0}+n_{\alpha1}$, $\mathbf{v}_\alpha(=\mathbf{v}_{\alpha0}+\mathbf{v}_{\alpha1})$ is the velocity, P_α is the pressure, and φ is the electric potential. In cylindrical coordinates $(r_\perp, \theta, z)$, the perturbation quantities $n_{\alpha1}(\mathbf{r}, t)$, $\mathbf{v}_\alpha(\mathbf{r}, t)$, and $\varphi(\mathbf{r}, t)$ would be written as the following wave-like dependence [17, 18]:

$$\begin{pmatrix} n_{\alpha1}(\mathbf{r}, t)\\ \mathbf{v}_{\alpha1}(\mathbf{r}, t)\\ \varphi(\mathbf{r}, t)\end{pmatrix}=\begin{pmatrix}\bar{n}_{\alpha1}(r_\perp)\\ \bar{\mathbf{v}}_{\alpha1}(r_\perp)\\ \bar{\varphi}(r_\perp)\end{pmatrix}\exp(-i\beta\theta)\exp[i(k_z z-\omega t)], \quad (6)$$

where $\bar{n}_{\alpha1}(r_\perp)$, $\bar{\mathbf{v}}_{\alpha1}(r_\perp)$, and $\bar{\varphi}(r_\perp)$ are the perturbation quantities in the transverse direction and $k_z[=(k^2-k_\perp^2)^{1/2}]$ is the propagation wave number along the axial z-direction of the cylindrical wave guide with the radius R, $k_\perp$ is the transverse wave number, and β is the separation constant for the azimuthal angle θ. Using Equations 2– 6, $\partial/\partial\theta=0$, and $\beta=0$, i.e. the azimuthally symmetric condition [18], and the plasma dielectric function $\varepsilon_{zz}(\omega, k_z)=\varepsilon_l(\omega, k_z)$ with two-temperature plasma electrons, the differential equation for the transverse potential field $\bar{\varphi}(r_\perp)$ is represented by

$$r_\perp^2\frac{\mathrm{d}^2\bar{\varphi}(r_\perp)}{\mathrm{d}r_\perp^2}+r_\perp\frac{\mathrm{d}\bar{\varphi}(r_\perp)}{\mathrm{d}r_\perp}+r_\perp^2\zeta^2(\omega, k_z)=0, \quad (7)$$

because the Laplacian ∇^2 is written as $\nabla^2=\nabla_\perp^2+\partial^2/\partial z^2$, where $\nabla_\perp^2$ is the transverse Laplacian and $\bar{n}_{\alpha1}(r_\perp)$, $\bar{\mathbf{v}}_{\alpha1}(r_\perp)$, and $\bar{\varphi}(r_\perp)$ are the perturbation quantities in the x-y plane, where $r_\perp$ is the radial distance in the x-y plane and the separation parameter $\zeta^2(\omega, k_z)$ is given by

$$\zeta^2(\omega,k_z)=-k_z^2\left[+\frac{1}{k_z^2\lambda_{\mathrm{H}}^2}-\frac{\omega_L^2}{\omega^2}\left(1+\frac{3k_z^2}{\omega^2}\frac{k_{\mathrm{B}}T_{\mathrm{L}}}{m_e}\right)-\frac{\omega_i^2}{\omega^2}\left(1+\frac{3k_z^2}{\omega^2}\frac{k_{\mathrm{B}}T_i}{m_i}\right)1-\frac{\omega_d^2}{\omega^2}\right]. \tag{8}$$

The general solution of Equation 7 is then obtained by $\bar{\varphi}(r_\perp)=a_1J_0(\zeta r_\perp)+a_2N_0(\zeta r_\perp)$, where $J_0(\zeta r_\perp)$ is the zeroth-order Bessel function of the first kind and $N_0(\zeta r_\perp)$ is the zeroth-order Neumann function, and a_1 and a_2 are constants. According to the boundary condition at the surface of the cylindrically bounded dusty plasma $r_\perp=R$ and the origin $r_\perp=0$, i.e. $a_2=0$ and $J_0(\zeta R)=0$, the parameter $\zeta^2(\omega, k_z)$ is determined by

$$\zeta^2(\omega,k_z)=\left(\frac{\mu_{0n}}{R}\right)^2, \tag{9}$$

where μ_{0n}(=2.4048, 5.5201, 8.6537, 11.7915, …) are the nth roots of the zeroth-order Bessel function of the first kind, i.e. $J_0(\mu_{0n})=0$. From Equations 8 and 9, the dispersion relation for the space-charge electron-acoustic wave in a cylindrically bounded dusty plasma of two-temperature electrons is then found to be

$$\left(\frac{\mu_{0n}}{k_zR}\right)^2+1+\frac{1}{k_z^2\lambda_{\mathrm{H}}^2}-\frac{\omega_L^2}{\omega^2}\left(1+\frac{3k_z^2}{\omega^2}\frac{k_{\mathrm{B}}T_{\mathrm{L}}}{m_e}\right)-\frac{\omega_i^2}{\omega^2}\left(1+\frac{3k_z^2}{\omega^2}\frac{k_{\mathrm{B}}T_i}{m_i}\right)-\frac{\omega_d^2}{\omega^2}=0. \tag{10}$$

3 Frequency and Group Velocity of Space-Charge Electron-Acoustic Wave

Because the dispersion relation for the space-charge electron-acoustic wave in a cylindrically bounded dusty plasma of two-temperature electrons (Equation 10) can be written as $A\omega^4-B\omega^2-C=0$, the stable frequency solution $\bar{\omega}_{\mathrm{SW}}(\equiv\omega/\omega_L)$ for the dispersion relation for the space-charge electron-acoustic wave in a cylindrically bounded dusty plasma of two-temperature electrons is then found to be

$$\begin{aligned}\bar{\omega}_{\mathrm{SW}}(\bar{k}_z,n_{\mathrm{H/L}},n_{i/\mathrm{L}},n_{d/\mathrm{L}},\bar{m},\bar{M},T_{\mathrm{H/L}},T_{i/\mathrm{L}},\mu_{0n},\bar{R})=\\ [B(n_i,n_{\mathrm{L}},n_d,m_e,m_i,m_d,Z_d)\\ +(B^2(n_i,n_{\mathrm{L}},n_d,m_e,m_i,m_d,Z_d)\\ +4A(\bar{k}_z,n_{\mathrm{H}},n_{\mathrm{L}},T_{\mathrm{H}},T_{\mathrm{L}},\mu_{0n},\bar{R})\\ C(\bar{k}_z,n_i,n_L,m_i,m_e,T_i,T_{\mathrm{L}}))^{1/2}]^{1/2}\\ /(2A(\bar{k}_z,n_{\mathrm{H}},n_{\mathrm{L}},T_{\mathrm{H}},T_{\mathrm{L}},\mu_{0n},\bar{R}))^{1/2},\end{aligned} \tag{11}$$

$$A(\bar{k}_z,n_{\mathrm{H}},n_{\mathrm{L}},T_{\mathrm{H}},T_{\mathrm{L}},\mu_{0n},\bar{R})=1+\frac{1}{\bar{k}_z^2}\left[\left(\frac{\mu_{0n}}{\bar{R}}\right)^2+\frac{n_{\mathrm{H/L}}}{T_{\mathrm{H/L}}}\right], \tag{12}$$

$$B(n_i,n_{\mathrm{L}},n_d,m_e,m_i,m_d,Z_d)=1+\frac{n_{i/\mathrm{L}}}{\bar{m}}+\frac{n_{d/\mathrm{L}}Z_d^2}{\bar{M}}, \tag{13}$$

and

$$C(\bar{k}_z,n_i,n_{\mathrm{L}},m_i,m_e,T_i,T_{\mathrm{L}})=3\bar{k}_z^2\left(1+\frac{n_{i/\mathrm{L}}T_{i/\mathrm{L}}}{\bar{m}^2}\right), \tag{14}$$

where $\omega_L[=(4\pi n_{\mathrm{L}}e^2/m_e)^{1/2}]$ is the electron plasma frequency for low-temperature electrons, n_{L} is the density of low-temperature electrons, $\bar{k}_z(\equiv k_z\lambda_{\mathrm{DL}})$ is the scaled propagation wave number, λ_{DL} is the Debye length for low-temperature electrons, $n_{\mathrm{H/L}}(\equiv n_{\mathrm{H}}/n_{\mathrm{L}})$ is the ratio of the density n_{H} of high-temperature electrons to the density n_{L} of low-temperature electrons, $n_{i/\mathrm{L}}(\equiv n_i/n_{\mathrm{L}})$ is the ratio of the density n_i of ions to the density n_{L} of low-temperature electrons, $n_{d/\mathrm{L}}(\equiv n_d/n_{\mathrm{L}})$ is the ratio of the density n_d of dust grains to the density n_{L} of low-temperature electrons, $\bar{m}(\equiv m_i/m_e)$ is the ratio of the ion mass m_i to the electron mass m_e, $\bar{M}(\equiv m_d/m_e)$ is the ratio of the dust mass m_i to the electron mass m_e, $T_{\mathrm{H/L}}(\equiv T_{\mathrm{H}}/T_{\mathrm{L}})$ is the ratio of the temperature T_{H} of high-temperature electrons to the temperature T_{L} of low-temperature electrons, $T_{i/\mathrm{L}}(\equiv T_i/T_{\mathrm{L}})$ is the ratio of the temperature T_i of ions to the temperature T_{L} of low-temperature electrons, and $\bar{R}(\equiv R/\lambda_{\mathrm{DL}})$ is the scaled radius of the cylindrical waveguide. The scaled group velocity of the space-charge electron-acoustic wave in a cylindrically bounded dusty plasma of two-temperature electrons would be then determined by $\bar{v}_{\mathrm{SW}}(=\mathrm{d}\bar{\omega}_{\mathrm{SW}}/\mathrm{d}\bar{k}_z)$:

$$\bar{v}_{\mathrm{SW}}(\bar{k}_z)=\frac{1}{2\bar{\omega}_{\mathrm{SW}}\sqrt{B^2+4AC}}\left(C\frac{\mathrm{d}A}{\mathrm{d}\bar{k}_z}+A\frac{\mathrm{d}C}{\mathrm{d}\bar{k}_z}\right)-\frac{\bar{\omega}_{\mathrm{SW}}}{2A}\frac{\mathrm{d}A}{\mathrm{d}\bar{k}_z}, \tag{15}$$

where the parameters A, B, and C are, respectively, given in Equations 12–14. Recently, the density and temperature effects [19] on a surface electron-acoustic wave are investigated in a semibounded dusty plasma of two-temperature electrons. However, the multimode dispersion characteristics of the space-charge wave have not been investigated in a cylindrical waveguide complex plasma, including two-temperature electrons. It would then be expected that the current results, i.e. Equations 11–15, are quite useful to investigate the physical properties of the frequency and the group velocity of the space-charge wave, including the density, temperature, and geometric effects. In recent years, the characteristics of quantum dusty plasmas have been extensively investigated because the quantum dusty plasma can be found in various nanomaterials, nanodevices, and semiconductor plasmas [20–28]. Very recently, the physical characteristics of space-charge waves in a warm plasma-filled elliptical waveguide in an infinite axial magnetic field are investigated [29]. Hence, the investigation of the space-charge quantum electron-acoustic wave in a cylindrically bounded quantum magneto dusty plasma of two-temperature quantum plasma electrons will be treated elsewhere. Recently, two kinds of streaming instabilities due to ion-streaming and dust-streaming are studied in the plasma system composed of a three-component electron-ion-dust quantum plasmas bounded by a cylindrical domain [18]. It is also shown that the streaming speeds, the boundary conditions, and the quantum parameters strongly influence the physical characteristics of instabilities [18] because of the boundary effect as well as the quantum effect. Hence, the stability of the space-charge wave in a cylindrically bounded streaming two-temperature plasma electrons will also be treated elsewhere.

4 Discussions

To explicitly investigate the physical characteristics of the space-charge electron-acoustic wave in a cylindrically bounded dusty plasma of two-temperature electrons, we assume that $\lambda_{\rm DL}=20a$, $Z_d=200$, and the mass density of the dust grain is $\rho_D \cong 2\ {\rm gm}^{-3}$, where a is the radius of the dust grain. Figure 1 shows the scaled frequency $\bar{\omega}_{\rm SW}(=\omega_{\rm SW}/\omega_{pi})$ of the space-charge wave in a cylindrically bounded dusty plasma of two-temperature electrons as a function of the scaled wave number $\bar{k}_z(=k_z\lambda_{\rm DL})$ along the axial z-axis for various values of the density ratio $n_{\rm H}/n_{\rm L}$ of electrons. From this figure, the frequency of the space-charge wave increases with an increase in the scaled wave number $\bar{k}_z$. As shown, it is found that the frequency $\bar{\omega}_{\rm SW}$ of the space-charge wave decreases with an increase in the density ratio $n_{\rm H}/n_{\rm L}$. Hence, we have found that the wave frequency $\bar{\omega}_{\rm SW}$ in a plasma with a high population of high-temperature electrons is always smaller than that in a plasma with a low population of high-temperature electrons. Figure 2 represents the space-charge plot of the scaled group velocity $\bar{v}_{\rm SW}(={\rm d}\bar{\omega}_{\rm SW}/{\rm d}\bar{k}_z)$ as a function of the scaled wave number $\bar{k}_z$ and the density ratio $n_{\rm H}/n_{\rm L}$. As shown in this figure, the group velocity $\bar{v}_{\rm SW}$ decreases with the increasing scaled wave number $\bar{k}_z$ and density ratio $n_{\rm H}/n_{\rm L}$. Hence, we have found that the population of high-temperature electrons suppresses the scaled group velocity $\bar{v}_{\rm SW}$ of the space-charge wave in a cylindrically bounded dusty plasma of two-temperature electrons. Figure 3 shows the surface plot of the scaled frequency $\bar{\omega}_{\rm SW}$ of the space-charge wave as a function of the scaled wave number $\bar{k}_z$ and the temperature ratio $T_{\rm H}/T_{\rm L}$. It is interesting to find out that the scaled frequency $\bar{\omega}_{\rm SW}$ of the space-charge wave is almost independent of the temperature variations of electrons. Figure 4 represents the surface plot of the scaled group velocity $\bar{v}_{\rm SW}$ of the space-charge wave as a function of the scaled wave number $\bar{k}_z$ and the temperature ratio $T_{\rm H}/T_{\rm L}$. From this figure, it is found that the scaled group velocity $\bar{v}_{\rm SW}$ increases with an increase in the temperature ratio $T_{\rm H}/T_{\rm L}$. Figure 5 shows the scaled frequency $\bar{\omega}_{\rm SW}$

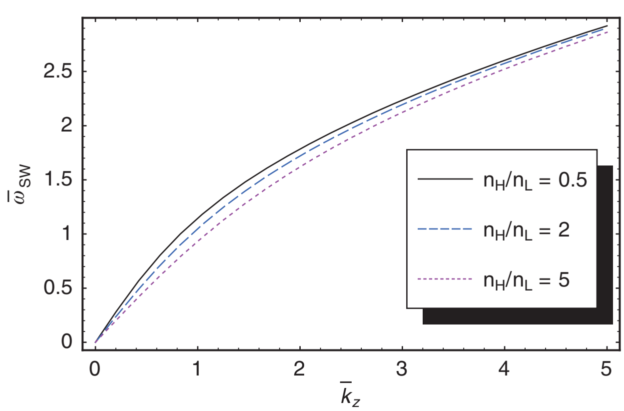

Figure 1: The scaled frequency $\bar{\omega}_{\rm SW}$ of the space-charge wave in a cylindrically bounded dusty plasma of two-temperature electrons as a function of the scaled wave number $\bar{k}_z(=k_z\lambda_{\rm DL})$ along the axial z-axis for the case of the first root μ_{01}(=2.4048) when $\bar{R}=3$, $T_{\rm H}/T_{\rm L}=2$, $n_i/n_{\rm L}=2$, $n_d/n_{\rm L}=0.1$, and $T_i/T_{\rm L}=1$. The solid line represents the case of $n_{\rm H}/n_{\rm L}=0.5$. The dashed line represents the case of $n_{\rm H}/n_{\rm L}=2$. The dotted line represents the case of $n_{\rm H}/n_{\rm L}=5$.

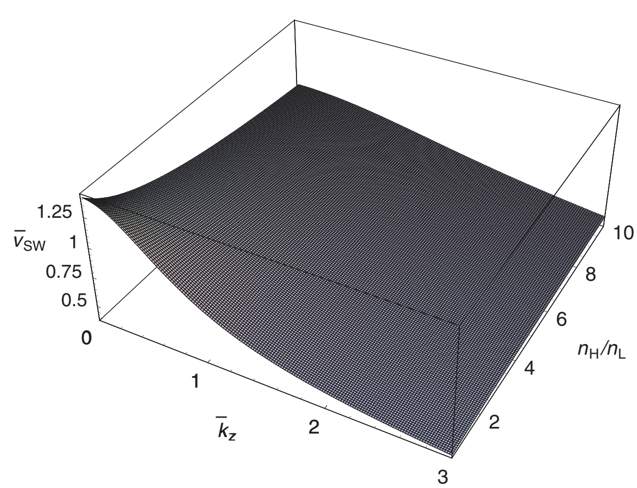

Figure 2: The surface plot of the scaled group velocity $\bar{v}_{\rm SW}$ as a function of the scaled wave number $\bar{k}_z$ and the density ratio $n_{\rm H}/n_{\rm L}$ for the case of the first root, i.e. μ_{01}(=2.4048) when $\bar{R}=3$, $T_{\rm H}/T_{\rm L}=2$, $n_i/n_{\rm L}=2$, $n_d/n_{\rm L}=0.1$, and $T_i/T_{\rm L}=1$.

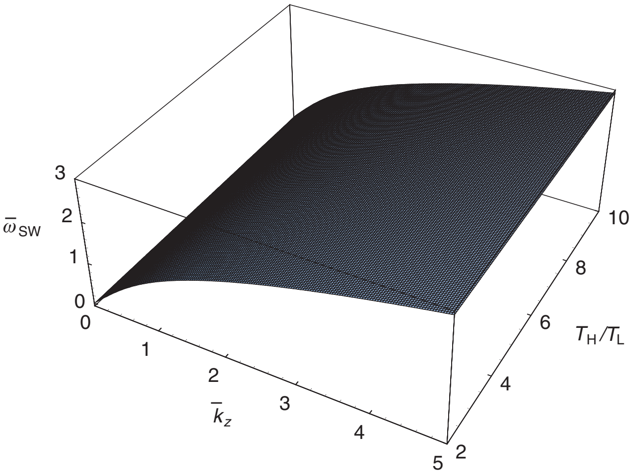

Figure 3: The surface plot of the scaled frequency $\bar{\omega}_{SW}$ of the space-charge wave as a function of the scaled wave number $\bar{k}_z$ and the temperature ratio T_H/T_L for the case of the first root μ_{01}(=2.4048) when $\bar{R}=3$, $n_H/n_L=0.5$, $n_i/n_L=2$, $n_d/n_L=0.1$, and $T_i/T_L=1$.

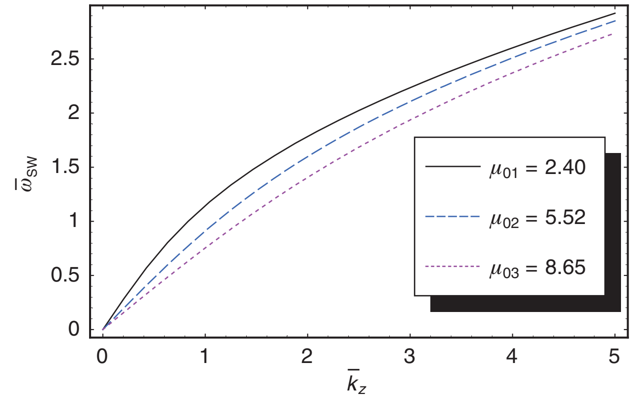

Figure 5: The scaled frequency $\bar{\omega}_{SW}$ of the space-charge wave as a function of the scaled wave number $\bar{k}_z$ when $\bar{R}=3$, $n_H/n_L=0.5$, $T_H/T_L=4$, $n_i/n_L=2$, $n_d/n_L=0.1$, and $T_i/T_L=1$. The solid line represents the case of the first root μ_{01}(=2.40). The dashed line represents the case of the second root μ_{02}(=5.40). The dotted line represents the case of the third root μ_{03}(=8.65).

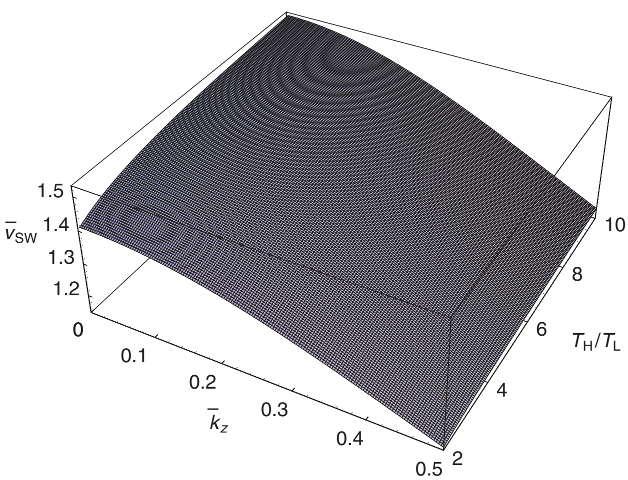

Figure 4: The surface plot of the scaled group velocity $\bar{v}_{SW}$ of the space-charge wave as a function of the scaled wave number $\bar{k}_z$ and the temperature ratio T_H/T_L. From this figure, it is found that the scaled group velocity $\bar{v}_{SW}$ increases with an increase of the temperature ratio T_H/T_L for the case of the first root μ_{01}(=2.4048) when $\bar{R}=3$, $n_H/n_L=0.5$, $n_i/n_L=2$, $n_d/n_L=0.1$, and $T_i/T_L=1$.

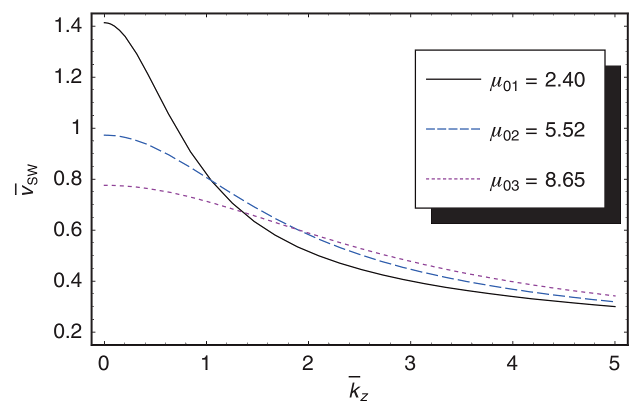

Figure 6: The scaled group velocity $\bar{v}_{SW}$ of the space-charge wave as a function of the scaled wave number $\bar{k}_z$ when $\bar{R}=3$, $n_H/n_L=0.5$, $T_H/T_L=4$, $n_i/n_L=2$, $n_d/n_L=0.1$, and $T_i/T_L=1$. The solid line represents the case of the first root μ_{01}(=2.40). The dashed line represents the case of the second root μ_{02}(=5.40). The dotted line represents the case of the third root μ_{03}(=8.65).

of the space-charge wave as a function of the scaled wave number $\bar{k}_z$ for various values the root of the zero-order Bessel function J_0. We find that the scaled frequency $\bar{\omega}_{SW}$ with the higher-order μ_{0p} of the root is smaller than that with the lower-order μ_{0q} of the root, i.e. $p>q$. Figure 6 plots the scaled group velocity $\bar{v}_{SW}$ of the space-charge wave as a function of the scaled wave number $\bar{k}_z$ for various values the root μ_{0p}, where the scaled group velocities $\bar{v}_{SW}$ with the higher-order μ_{0p} of the root are smaller for $0<\bar{k}_z<1$ and larger for $\bar{k}_z>1$ than those with the lower-order μ_{0q} of the root. Figure 7 represents the scaled frequency $\bar{\omega}_{SW}$ of the space-charge wave as a function of the scaled radius $\bar{R}$ of the cylindrical wave guide for various values the root μ_{0p}. From this figure, we find that the scaled frequency $\bar{\omega}_{SW}$ increases with an increase in the scaled radius $\bar{R}$, whereas the influence of root order on the frequency $\bar{\omega}_{SW}$ decreases with increasing scaled radius $\bar{R}$. Figure 8 shows the scaled group velocity $\bar{v}_{SW}$ of the space-charge wave as a function of the scaled radius $\bar{R}$ for various values the root. We note that the scaled group velocity $\bar{v}_{SW}$ decreases with increasing scaled radius $\bar{R}$. It is also found that the influence of root order on the group velocity $\bar{v}_{SW}$ decreases with an increase in the scaled radius $\bar{R}$.

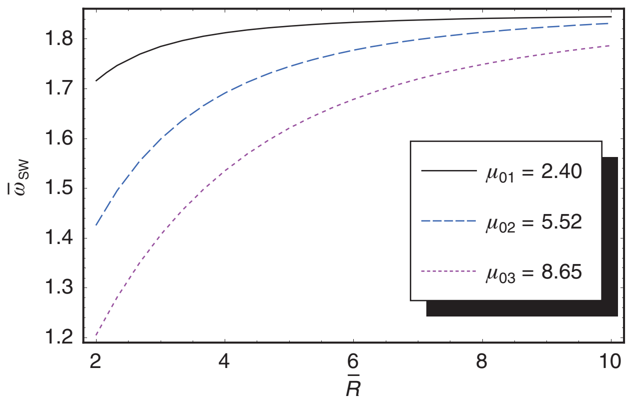

Figure 7: The scaled frequency $\bar{\omega}_{SW}$ of the space-charge wave as a function of the scaled radius $\bar{R}$ when $\bar{k}_z = 2$, $n_H/n_L = 0.5$, $T_H/T_L = 4$, $n_i/n_L = 2$, $n_d/n_L = 0.1$, and $T_i/T_L = 1$. The solid line represents the case of the first root μ_{01}(=2.40). The dashed line represents the case of the second root μ_{02}(=5.40). The dotted line represents the case of the third root μ_{03}(=8.65).

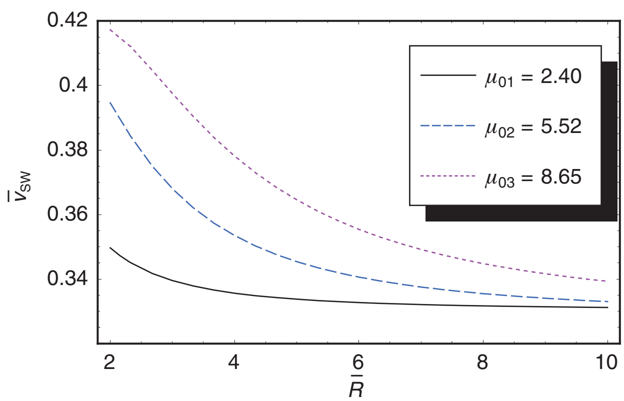

Figure 8: The scaled group velocity $\bar{v}_{SW}$ of the space-charge wave as a function of the scaled radius $\bar{R}$ when $\bar{k}_z = 2$, $n_H/n_L = 0.5$, $T_H/T_L = 4$, $n_i/n_L = 2$, $n_d/n_L = 0.1$, and $T_i/T_L = 1$. The solid line represents the case of the first root μ_{01}(=2.40). The dashed line represents the case of the second root μ_{02}(=5.40). The dotted line represents the case of the third root μ_{03}(=8.65).

5 Conclusion

In this work, we investigated the multimode characteristics of the space-charge wave in a cylindrical waveguide complex plasma. The dispersion relation of the space-charge wave is derived in a waveguide, including two-temperature electrons. The results show that the wave frequencies in a plasma with a high population of high-temperature electrons are always smaller those in a plasma with a low population of high-temperature electrons. It is also found that the population of high-temperature electrons suppresses the group velocity of the space-charge wave. It is interesting to find out that the frequency of the space-charge wave is almost independent of the temperature variations of electrons. It is also found that the group velocity increases with an increase in the ratio of the temperature of hot electrons to the temperature of cold electrons. It is also found that the frequency with the higher-order root is smaller than that with the lower-order root. In addition, it is found that the frequency increases with an increase in the radius of the cylindrical wave guide. From this work, we have shown that the influence of plasma density and temperature plays a crucial role in the propagation of the space-charge electron-acoustic wave in a cylindrically bounded dusty plasma of two-temperature electrons. These results would provide useful information on the physical characteristics of space-charge waves in bounded bi-Maxwellian dusty plasmas consisting of two-electron-species.

Acknowledgments: This paper is dedicated to the late Prof. P. K. Shukla in memory of exciting and stimulating collaborations on physical processes in dusty plasmas. One of the authors (Y.-D.J.) gratefully acknowledges Dr. M. Rosenberg for useful discussions and warm hospitality while visiting the Department of Electrical and Computer Engineering at the University of California, San Diego. This research was initiated while one of the authors (Y.-D.J.) was affiliated with University of California, San Diego, as a visiting professor. This research was supported by the Basic Science Research Program through the National Research Foundation of Korea (NRF) funded by the Ministry of Education, Science and Technology (grant no. 2012-001493).

References

[1] A. F. Alexandrov, L. S. Bogdankevich, and A. A. Rukhadze, Principles of Plasma Electrodynamics, Springer, Berlin, 1984.
[2] Yu. M. Aliev, H. Schlüter, and A. Shivarova, Guided-Wave-Produced Plasmas, Springer, Berlin, 2000.
[3] V. Girka, I. Girka, and M. Thumm, Surface Flute Waves in Plasmas, Springer, Cham, 2014.
[4] F. B. Baimbetov, Kh. T. Nurekenov, and T. S. Ramazanov, Phys. Lett. A **202**, 211 (1995).
[5] H. F. Beyer and V. P. Shevelko, Introduction to the Physics of Highly Charged Ions, Institute of Physics, Bristol, 2003.
[6] D. A. Mendis and M. Rosenberg, Ann. Rev. Astron. Astrophys. **32**, 419 (1994).
[7] P. Bliokh, V. Sinitsin, and V. Yaroshenko, Dusty and Self-Gravitational Plasma in Space, Kluwer, Dordrecht, 1995.
[8] A. Bouchoule, Dusty Plasmas: Physics, Chemistry and Technological Impacts in Plasma Processing, Wiley, Chichester, 1999.
[9] P. K. Shukla and A. A. Mamum, Introduction to Dusty Plasma Physics, Institute of Physics Publishing, Bristol, 2002.

[10] W. D. Jones, A. Lee, S. M. Gleman, and H. J. Doucetf, Phys. Rev. Lett. **35**, 1349 (1975).
[11] B. N. Goswami and B. Buti, Phys. Lett. A **57**, 149 (1976).
[12] K. Baumgärtel, Ann. Geophys. **32**, 1025 (2014).
[13] K. Watanabe and T. Taniuti, J. Phys. Soc. Jpn. **43**, 1819 (1977).
[14] S. Peter and R. L. Tokar, Phys. Fluids. **28**, 2439 (1985).
[15] W. Baumjohann and R. A. Treumann, Basic Space Plasma Physics, Imperial College Press, Singapore, 1996.
[16] P. M. Bellan, Fundamentals of Plasma Physics, Cambridge University Press, Cambridge, 2006.
[17] N. A. Krall and A. W. Trivelpiece, Principles of Plasma Physics, McGraw-Hill, New York, 1973.
[18] K.-Z. Zhang and J.-K. Xue, Phys. Plasmas **17**, 032113 (2010).
[19] D.-H. Ki and Y.-D. Jung, J. Plasma Phys. **73**, 433 (2007).
[20] M. Jamil, M. Shahid, W. Ali, M. Salimullah, H. A. Shah, and G. Murtaza, Phys. Plasmas **18**, 063705 (2011).
[21] M. Akbari-Moghanjoughi, Phys. Plasmas **19**, 032703, 2012 (2012).
[22] M. Akbari-Moghanjoughi, J. Plasma Phys. **79**, 189 (2013).
[23] M. Jamil, Z. Mir, M. Asif, and M. Salimullah, Phys. Plasmas **21**, 092111 (2014).
[24] M. Akbari-Moghanjoughi, Phys. Plasmas **22**, 022103 (2015).
[25] W.-P. Hong, M. Jamil, A. Rasheed, and Y.-D. Jung, Z. Naturforsch. **70a**, 413 (2015).
[26] A. A. Khan, M. Jamil, and A. Hussain, Phys. Plasmas **22**, 092103, 2015 (2015).
[27] Z. Moldabekov, T. Schoof, P. Ludwig, M. Bonitz, and T. Ramazanov, Phys. Plasmas **22**, 102104 (2015).
[28] A. Rasheed, M. Jamil, F. Areeb, M. Siddique, M. Salimullah, J. Phys. D **49**, 175109 (2016).
[29] A. Abdoli-Arani and S. Safari, Wave Random Complex **25**, 259 (2015).